Bioorganic Chemistry 82 (2019) 6–16

Contents lists available at ScienceDirect

Bioorganic Chemistry

journal homepage: www.elsevier.com/locate/bioorg

Acridine-based (thio)semicarbazones and hydrazones: Synthesis, *in vitro* urease inhibition, molecular docking and *in-silico* ADME evaluation

Ibanga Okon Isaac[a], Mariya al-Rashida[b], Shafiq Ur Rahman[c], Rima D. Alharthy[d], Asnuzilawati Asari[e], Abdul Hameed[a,*], Khalid Mohammed Khan[a,f], Jamshed Iqbal[c,*]

[a] *H. E. J. Research Institute of Chemistry, International Center for Chemical and Biological Sciences, University of Karachi, Karachi 75270, Pakistan*
[b] *Department of Chemistry, Forman Christian College (A Chartered University), Ferozepur Road, Lahore 54600, Pakistan*
[c] *Center for Advanced Drug Research, COMSATS Institute of Information Technology, Abbottabad 22060, Pakistan*
[d] *Department of Chemistry, Science and Arts College, Rabigh Campus, King Abdulaziz University, Jeddah, Saudi Arabia*
[e] *School of Fundamental Science, Universiti Malaysia Terengganu, 21030 Kuala Nerus, Terengganu, Malaysia*
[f] *Department of Clinical Pharmacy, Institute for Research and Medical Consultations (IRMC), Imam Abdulrahman Bin Faisal University, P.O. Box 31441, Dammam, Saudi Arabia*

ARTICLE INFO

Keywords:
(Thio)semicarbazones
Urease inhibition
Pathogenic bacteria
Acridine
In silico ADME

ABSTRACT

Urease is a bacterial enzyme that is responsible for virulence of various pathogenic bacteria such as *Staphylococcus aureus, Proteus mirabilis*, *Klebsiella pneumoniae*, *Ureaplasma urealyticum*, *Helicobacter pylori* and *Mycobacterium tuberculosis*. Increased urease activity aids in survival and colonization of pathogenic bacteria causing several disorders especially gastric ulceration. Hence, urease inhibitors are used for treatment of such diseases. In search of new molecules with better urease inhibitory activity, herein we report a series of acridine derived (thio)semicarbazones (**4a-4e**, **6a-6l**) that were found to be active against urease enzyme. Molecular docking studies were carried out to better comprehend the preferential mode of binding of these compounds against urease enzyme. Docking against urease from pathogenic bacterium *S. pasteurii* was also carried out with favorable results. *In silico* ADME evaluation was done to determine drug likeness of synthesized compounds.

1. Introduction

Urease (E.C. 3.5.1.5) is a nickel containing metalloenzyme that is commonly found in bacteria, algae, fungi and plants. It is responsible for catalytic hydrolysis of urea to ammonia and carbamate, which quickly hydrolyzes to ammonia and carbonic acid. Urease is responsible for pathogenesis of several bacteria, well-known among these include *Staphylococcus aureus, Proteus mirabilis*, *Klebsiella pneumoniae*, *Ureaplasma urealyticum*, *Helicobacter pylori* and *Mycobacterium tuberculosis* [1–3]. A number of bacterial infections are characterized by an increased ureolytic activity, a hallmark of urease enzyme. In humans the urease enzyme is recognized as immunogenic in nature, and prolonged exposure to urease can trigger release of antibodies which, in some cases, may lead to inflammation [4]. Urease is also responsible for damage to epithelial cells, since it stimulates neutrophils and monocytes, leading to secretion of inflammatory cytokines [5]. The urease enzyme plays an essential role in survival and colonization of bacterial pathogens. By virtue of its ureolytic activity, urease enzyme increases the concentration of ammonia in its microenvironment, high concentration of ammonia results in basic pH and protects the bacterial colony from the gastric acid. Urease activity has been recognized as a virulence factor for *H. pylori* infections including gastritis and peptic ulceration, whereby the basic pH around the bacteria, due to bacterial urease activity, protects the bacteria and also helps in its colonization in the acidic environment of the stomach [6]. Studies have shown that *H. pylori* urease negative mutants are incapable of colonization [7]. *H. Pylori* infection is responsible for many gastroduodenal disorders. If left untreated, or not treated properly, the infection can turn into chronic gastritis increasing the risk of peptic ulcers and gastric cancer [8,9]. Increased urease activity (as a result of pathogenesis) is also responsible for alkalization of urine in human host. Due to an increase in urine pH, precipitation of (otherwise soluble) struvite and carbonate apatite occurs around the bacteria resulting in formation of urinary stones. This urinary stone formation further protects the pathogenic bacteria from the effects of antibiotics and also helps these pathogenic bacteria to evade the host's immune responses [10–12]. The combination of

* Corresponding authors.
E-mail addresses: abdul_hameed8@hotmail.com (A. Hameed), drjamshed@ciit.net.pk (J. Iqbal).

https://doi.org/10.1016/j.bioorg.2018.09.032
Received 10 July 2018; Received in revised form 19 September 2018; Accepted 21 September 2018
Available online 22 September 2018
0045-2068/

antibiotic therapy with rease inhibitors has long been deemed beneficial for the treatment of kidney stones and urease positive urinary tract infections [13–15].

These observations demand the discovery of new and potent inhibitors of urease. Several classes of compounds have been reported as urease inhibitors. The most well-known among these are hydroxamic acid and its derivatives [16,17]. However the mutagenic properties of these hydroxamic acid derivatives have prevented their clinical development [18]. Phosphorodiamidates are also well-known inhibitors of urease [19], however their clinical exploitation has been encumbered due to their degradation at low pH [20]. Other classes of compounds with urease inhibitory activity include a variety of Schiff bases and their metal complexes [21], and a variety of urea/thiourea derived compounds [22,23]. Moreover, the (thio)semicarbazones [24,25], *N*-phenyl thiosemicarbazones [26], hydrazones [27] and (thio)urea [28] possessing close similitude with urea/thiourea moiety also showed urease inhibitory activity. Acridine derivatives are well-known and versatile chemotherapeutic agents. They have long been known for their outstanding antimicrobial activities, although more recently, most of the focus on acridine derivatives has been shifted to their anticancer activity, by virtue of their ability to intercalate DNA and bind with topoisomerase [29,30]. In the continuation of our interest in (thio)semicarbazones based molecule as urease inhibitors [24,26,31], Herein, we report novel acridine based (thio)semicarbazones and hydrazones as potent inhibitors of urease enzyme (Fig. 1).

2. Results and discussion

2.1. Chemistry

The desired acridine-based (thio)semicarbazones (**4a-4e**) and hydrazones (**6a-6l**) bearing acridines moieties were prepared by following the Scheme 1. The acridine scaffold **2** was prepared by the reaction of dimedone, benzaldehyde and ammonium acetate by using nickel (II) fluoride tetrahydrate as catalyst in ethanol as solvent. The intermediate **2** was then treated with hydrazine hydrate and subsequently reacted with substitute phenylisocyanate or phenyl isothiocyanate in the presence of protonated acid i.e. acetic acid to afford the corresponding products (**4a-4e**) in 50–75% yield [32]. Moreover, the different substituted acridine scaffolds were also reacted with 2,4-dinitrophenyl hydrazine in the presence of acetic acid to afford the series acridine-based hydrazone (**6a-6l**) in 71–99% yield. The detailed spectral data of all compounds have been provided in the experimental section.

The proton (^{1}H) NMR of a typical acridine-based semicarbazone **4a** showed characteristic broad singlet (brs) for 2N*H*^{a}, 2N*H*^{b}, and N*H* at δ_H 8.75, 9.35 and 8.43, respectively. The singlet of methine (C*H*^{9}) group appeared at δ_H 5.38, while the aromatic peaks of fourteen protons was found between δ_H 7.84–6.95. The singlet (brs) for characteristic aromatic proton (Ar*H*$^{2'}$/$^{2'}$) appeared at δ_H 7.84. Further in the ^{1}H NMR spectrum, the four methylene groups appeared as two separate triples, each with integration of four protons, at δ_H 2.30 and 2.09, respectively.

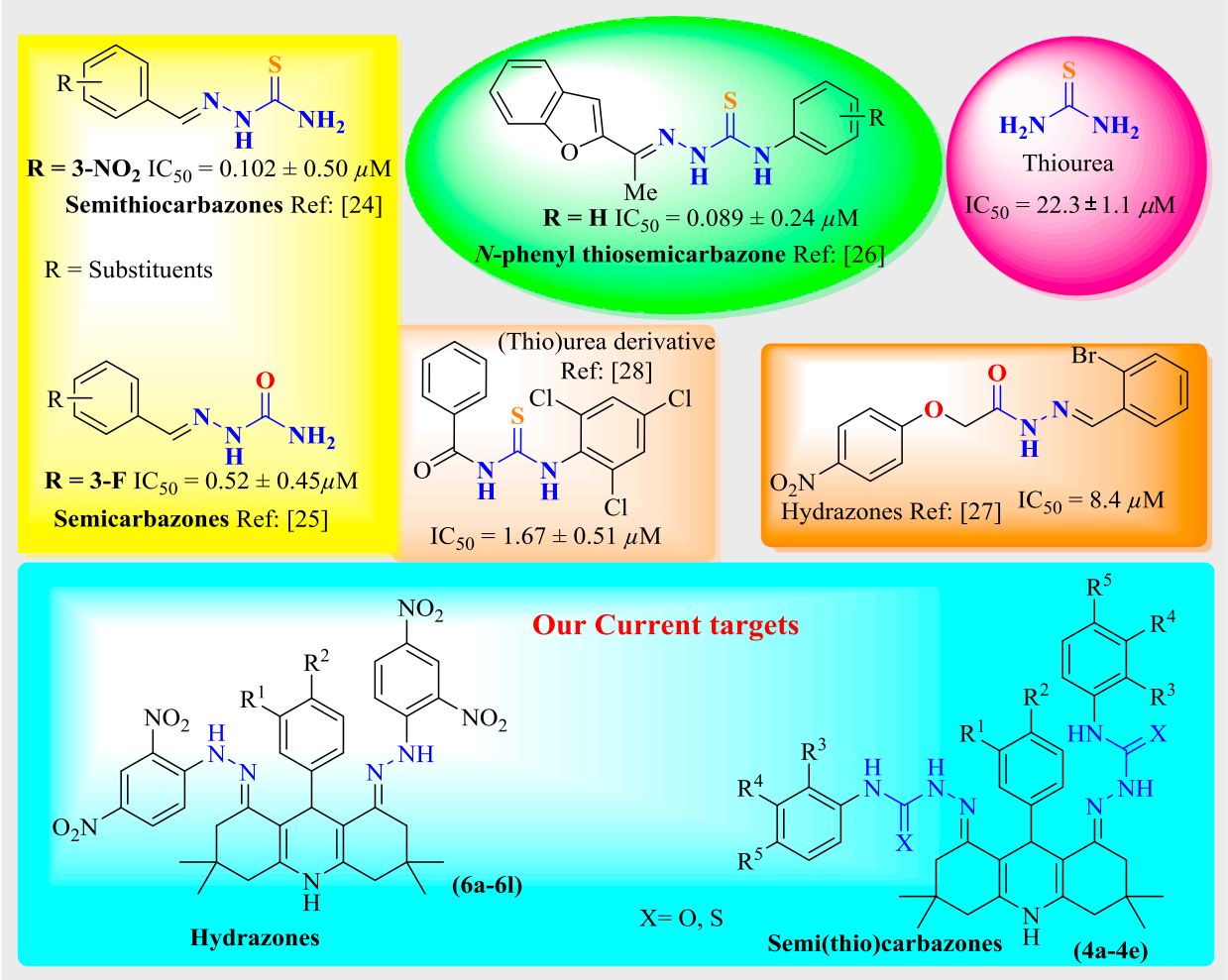

Fig. 1. Structure of reported (thio)semicarbazones, hydrazones and our acridine-(thio)semicarbazones/-hydrazones.

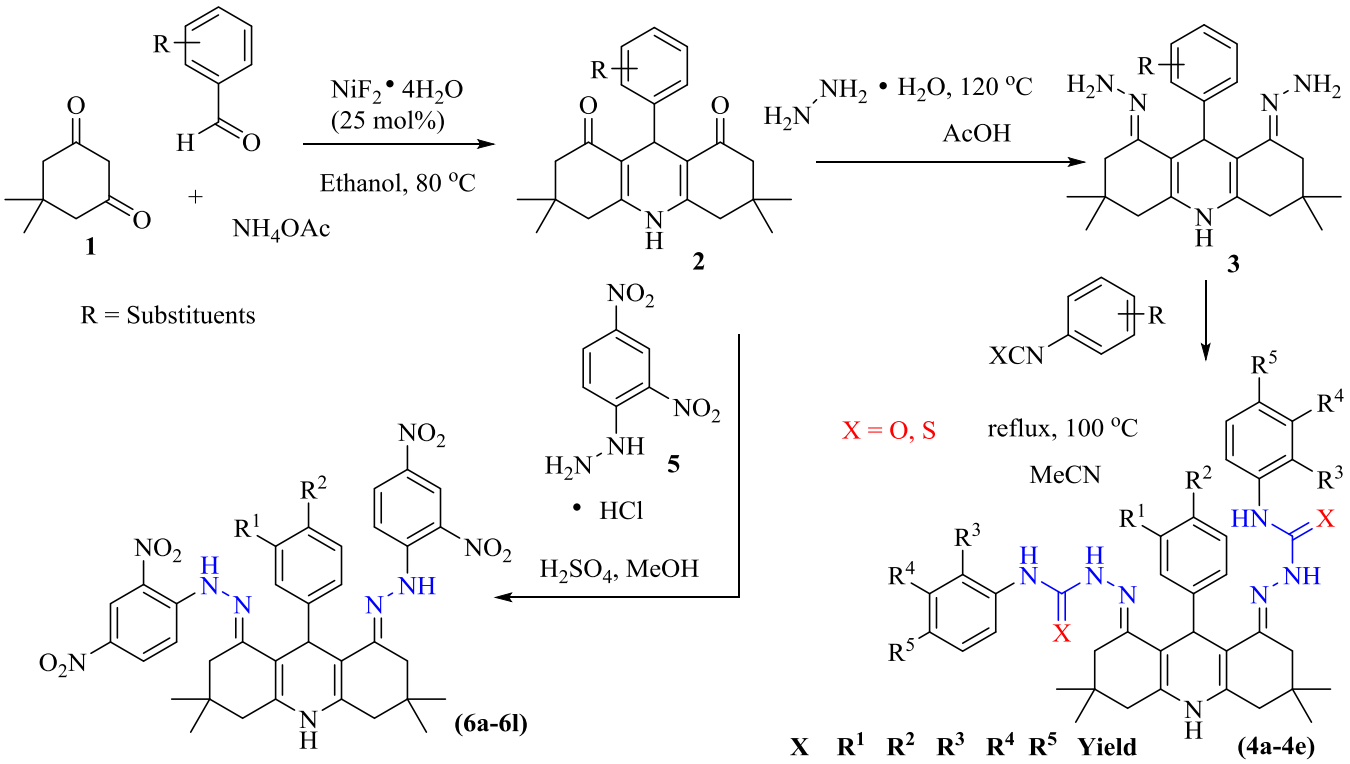

	R^1	R^2	Yield		R^1	R^2	Yield
6a	H	Me	96%	**6g**	OMe	F	97%
6b	OH	H	85%	**6h**	OMe	H	86%
6c	H	F	78%	**6i**	H	OMe	82%
6d	Br	OMe	85%	**6j**	H	OH	99%
6e	H	Cl	75%	**6k**	Cl	H	76%
6f	H	SMe	71%	**6l**	F	H	81%

	X	R^1	R^2	R^3	R^4	R^5	Yield
4a	O	H	H	H	Cl	H	63%
4b	O	H	Cl	H	Cl	H	50%
4c	S	OH	H	H	H	H	60%
4d	S	OH	H	F	H	H	76%
4e	S	H	Me	H	H	H	74%

Scheme 1. General scheme of synthesis for acridine-based (thio)semicarbazones **4a-4e** and hydrazones **6a-6l**.

The singlets of four methyl groups at positions C-3/6 appeared at δ_H 1.03 (CH_3 × 2) and 0.82 (CH_3 × 2), respectively (see supplementary information). Other spectroscopic data include IR and mass spectra results have been provided in the experimental section.

3. Bioactivity

3.1. Urease inhibition and Structure-Activity Relationship (SAR)

All the synthetic compounds **4a-4e** and **6a-6l** were evaluated for their *in vitro* urease inhibitory activity. All compounds were able to inhibit urease activity (IC_{50} values are in the range 20.1–43 μM). Many compounds were found to be even more active than the standard inhibitor thiourea (IC_{50} = 22.3 ± 1.1 μM). The urease inhibitory activities of compounds containing (thio)urea linkages (**4a-4e**) were in the IC_{50} range 20.1–36.3 μM, whereas for acridine derivatives containing hydrazone linkages (**6a-6l**), the IC_{50} values were in the range 20.3–43 μM. Among the two series of compounds, overall acridine derivatives containing (thio)urea linkages (**4a-4e**) were more active urease inhibitors as compared to acridine derivatives containing hydrazone linkages (**6a-6l**). Urease inhibitory activities of compounds from both series **4a-4e** and **6a-6l** are given in Tables 1 and 2, respectively.

Among compounds containing (thio)urea linkages (**4a-4e**), the compounds containing thiourea derived linkage were more active than urea containing analogs. Compound **4e** containing a thiourea linkage was found to be the most active urease inhibitor (IC_{50} = 20.1 ± 1.7 μM) and was slightly more active than the standard inhibitor thiourea (IC_{50} = 22.3 ± 1.1 μM). As compared to compound **4a**, all substitutions on the phenyl rings attached to the (thio)urea linkage, lead to a decrease in urease inhibitory activity, indicating that

Table 1
Urease inhibitory activities of compounds **4a-4e**.

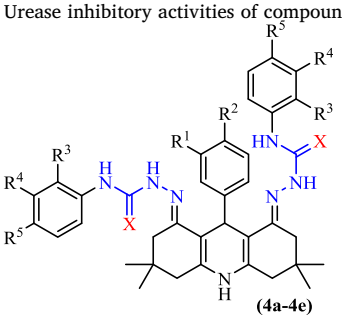

Entry	Compounds	X	R^1	R^2	R^3	R^4	R^5	IC_{50} ± SEM (μM)
1	**4a**	O	H	H	H	Cl	H	27.7 ± 2.4
2	**4b**	O	H	Cl	H	Cl	H	32.7 ± 3.1
3	**4c**	S	OH	H	H	H	H	36.3 ± 3.5
4	**4d**	S	OH	H	F	H	H	34.3 ± 3.0
5	**4e**	S	H	Me	H	H	H	20.1 ± 1.7
Reference	**Thiourea**							22.3 ± 1.1

Table 2
Urease inhibitory activities of compounds **6a-6l**.

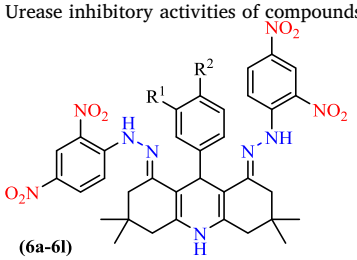

(6a-6l)

Entry	Compounds	R^1	R^2	IC_{50} ± SEM (μM)
9	**6a**	H	Me	43.0 ± 3.9
10	**6b**	OH	H	36.6 ± 3.1
11	**6c**	H	F	26.4 ± 2.1
12	**6d**	Br	OMe	20.3 ± 1.8
13	**6e**	H	Cl	41.0 ± 3.8
14	**6f**	H	SMe	28.0 ± 1.9
15	**6g**	OMe	F	33.0 ± 2.9
17	**6h**	OMe	H	33.1 ± 3.0
18	**6i**	H	OMe	26.5 ± 2.2
19	**6j**	H	OH	33.7 ± 2.9
20	**6k**	Cl	H	24.2 ± 1.8
21	**6l**	F	H	32.4 ± 3.1
Reference	**Thiourea**			22.3 ± 1.1

substitution on these phenyl rings does not contribute favorably to binding with the enzyme. Among compounds containing these substituted phenyl(thio)urea moieties, compound **4a** containing *m*-chlorophenyl urea group, a slight decreased activity was observed (IC_{50} = 27.7 ± 2.4 μM). Substitution on phenyl ring at 9-position of acridine ring was similarly found to lead to a decreased activity, as seen in compound **4b** (IC_{50} = 32.7 ± 3.1 μM) which is identical in structure to **4a,** with an additional *p*-Cl substituent on the phenyl ring at 9-position of the acridine ring. Compared to **4d**, compound **4e** has significantly reduced activity (Fig. 2).

Same trend was observed for compounds containing thiourea linkages. Compound **4e** is the most active inhibitor in the series bearing *p*-Me group substituted at phenyl ring at 9-position of the acridine ring (Fig. 2). Compared to **4e**, the activity of **4c** is drastically reduced (IC_{50} = 36.3 ± 3.5 μM) as *m*-OH substituent is introduced on the phenyl ring at 9-position of acridine ring. This clearly indicates that substitution at any of the phenyl rings of acridine ring leads to a decreased urease inhibition. Similarly, the compound **4d** having *m*-OH substituent on phenyl ring at 9-position of acridine ring exhibits significantly less urease inhibitory activity of **4g** (IC_{50} = 34.3 ± 3.0 μM) (Fig. 3).

Among acridine derived hydrazone derivatives (**6a-6l**), compound **6d** containing *m*-Br and *p*-OMe groups substituted on phenyl ring at 9-position of acridine ring, was found to be most active inhibitor (IC_{50} = 20.3 ± 1.8 μM). However, for similar compound **6g,** containing *m*-OMe and *p*-F groups substituted on phenyl ring at 9-position of acridine ring, a significant decrease in inhibitory activity was observed (IC_{50} = 33.0 ± 2.9 μM), indicating the importance of a halogen substituent at *m*-position and alkoxy substituent at *p*-position of phenyl ring for effective urease inhibition (Fig. 4).

With only one exception (compound **6e**), substitution at *para* position of phenyl ring at 9-position of acridine ring, leads to increase in urease inhibitory activity. Hence compound **6j** containing *p*-OH-Ph group was moderately more active (IC_{50} = 33.7 ± 2.9 μM) than its *m*-OH-Ph isomer compound **6b** (IC_{50} = 36.6 ± 3.1 μM). Similarly, the *p*-F-Ph containing compound **6c** was much more active inhibitor (IC_{50} = 26.4 ± 2.1 μM) as compared to its *m*-F-Ph analog compound **6l** (IC_{50} = 32.4 ± 3.1 μM). Same trend was observed for compound **6i** which contained a *p*-OMe-Ph, and was significantly more active (IC_{50} = 26.5 ± 2.2 μM) than its *m*-OMe-Ph analog, compound **6h** (IC_{50} = 33.1 ± 3.0 μM). Compound **6e** containing *p*-Cl-Ph group was the only exception to this trend; **6e** was significantly less active (IC_{50} = 41.0 ± 3.8 μM) as compared to its *m*-Cl-Ph analog **6k** (IC_{50} = 24.2 ± 1.8 μM) Fig. 5

Compared to compound **6i** containing *p*-OMe-Ph group (IC_{50} = 26.5 ± 2.2 μM), the inhibitory activity of its structural analog **6f** containing *p*-OMe-Ph group, was found to be slightly decreased (IC_{50} = 28.0 ± 1.9 μM). However, this S/OMe group is changed to Me group, as in compound **6a** a significant decrease in inhibitory activity was observed (IC_{50} = 43.0 ± 3.9 μM). In fact, compound **6a** was the least active inhibitor in the series. This indicates that non-alkylated phenyl substituents are preferable for effective urease inhibition from this class of compounds.

4. Molecular docking

Molecular docking studies were carried out to rationalize most probable enzyme-ligand binding interactions. Crystal structure of jack bean urease was downloaded from the PDB (PDB id: 4GY7 at 1.49 Å resolution). Prior to docking structures of ligands were optimized using semi empirical PM3 methods in HyperChem. Molecular docking was carried out using BioSolveIT's LeadIT software [34] which makes use of versatile FlexX method. Fig. 6 shows most probable docked conformation of most active urease inhibitor **4e**. All compounds were found to have similar binding modes, and were found to bind at the entrance of the active site. Due to the bulky nature of compounds, they were found to have a snug fit at the entrance of the active site cavity, interactions with the neighboring amino acids serve to stabilize the enzyme-inhibitor complex, thereby possibly preventing the substrate entry and

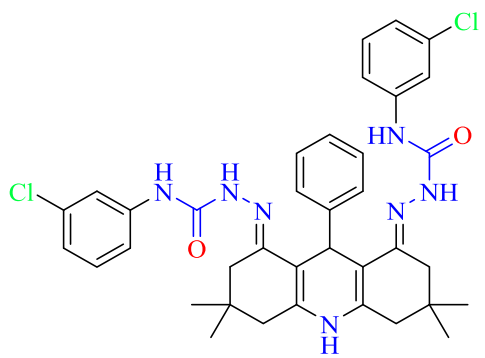

4a (IC_{50} = 27.7 ± 2.4 μM)

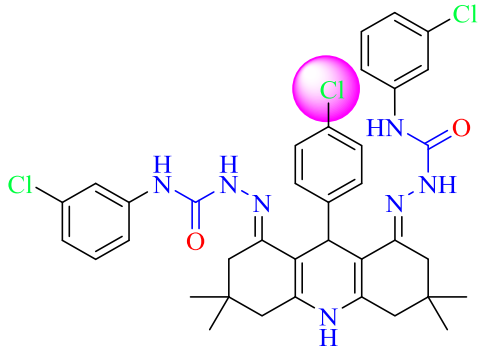

4b (IC_{50} = 32.7 ± 3.1 μM)

Fig. 2. Structure activity relationship for compounds **4a** and **4b**, indicating decrease in urease inhibitory activity as the phenyl ring on acridine ring is substituted at *p*-position.

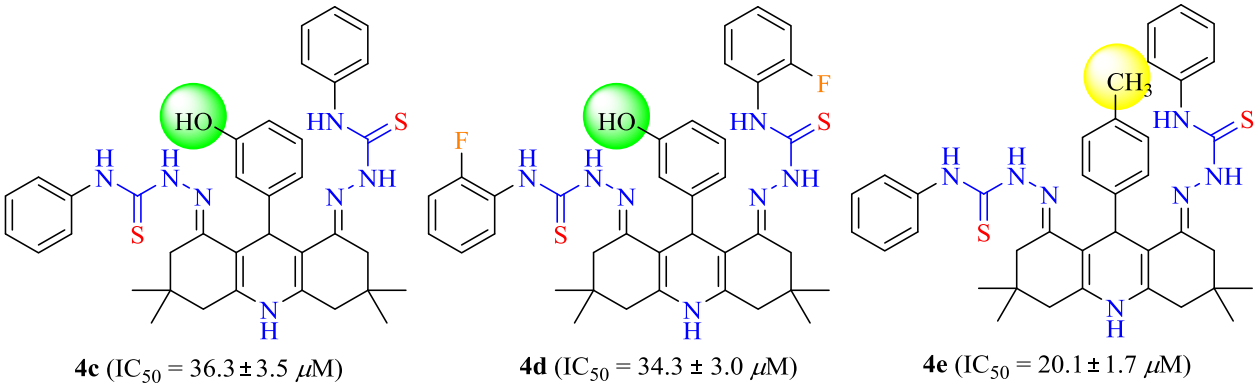

Fig. 3. Structure activity relationship of compound **4c** as compared to compound **4e**.

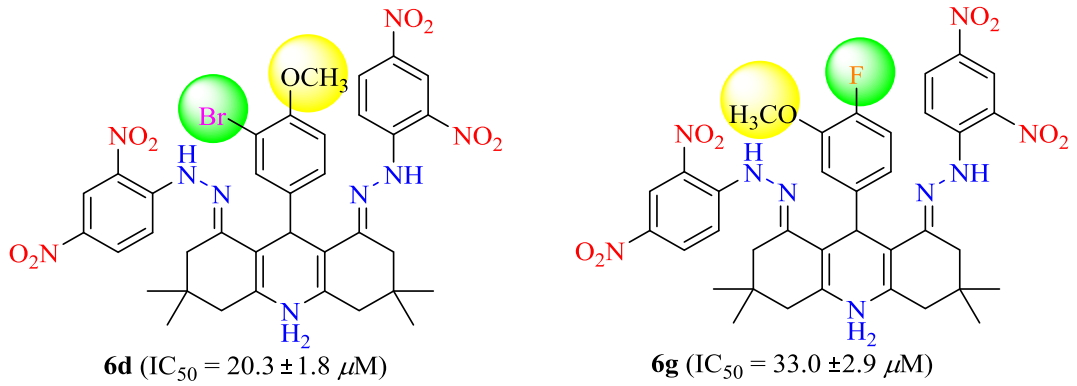

Fig. 4. Structure activity relationship for compounds **6d** and **6g**, indicating the importance of a halogen substituent at *m*-position and alkoxy substituent at *p*-position of phenyl ring for effective urease inhibition.

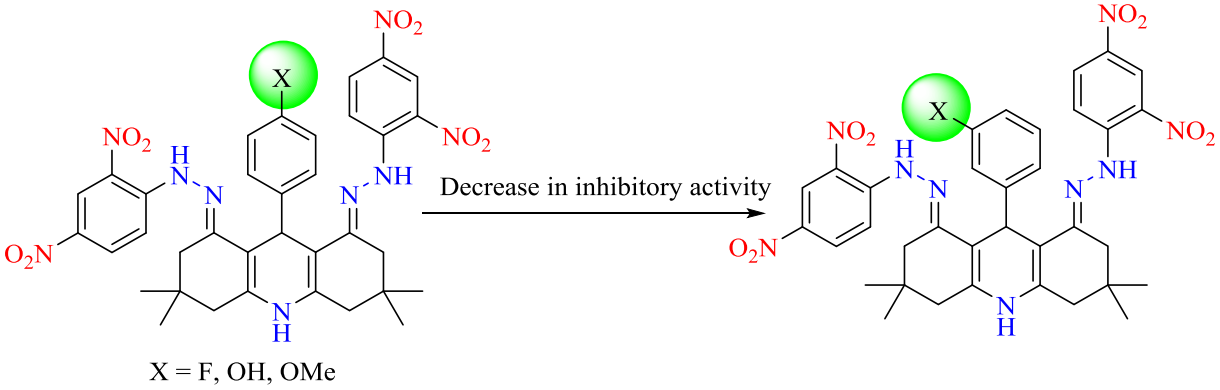

Fig. 5. Structure activity relationship for compounds **6c**, **6j**, **6i**, indicating a decrease in inhibition activity as the position of substituents is changed from *p*- to *m*- for compounds **6l**, **6b**, **6h**).

binding at the active site. One of the amino (−NH−) groups of the thiourea linkage was making a hydrogen bonded interaction with His593. The NH group of second thiourea linkage was acting as a hydrogen bond donor towards Asp494.

From second series of compounds (**6a-6l**), compound **6d** was found to be the most active inhibitor (20.3 ± 1.8 μM). Fig. 7 shows 3D and 2D interactions of most probable docked conformation of **6d** against urease enzyme. Similar to **4e**, compound **6d** was also found to bind near the entrance of the active site cavity, although with slightly diffeent onformation than that observed for compound **4e**. Unlike compound **4e**, where the acridine ring nitrogen atoms makes a hydrogen bond with His594, in compound **6d** there is no such interaction; instead one of the nitro group is involved in making hydrogen bond contact with His594. The other nitro group is making hydrgen bond with Arg439 and Cme592 (carboxymethylated cysteine). Fig. 8 shows overlap of compounds **4e** and **6d** in active site cavity of urease. As can be seen from the figure, due to the bulky nature of inhibitors, they bind at the entrance of the active site cavity, thereby interfering either with substrate binding or subsequent product release. Molecular docking against pathogenic bacterial urease (*S. pasteurii*) were also carried out. The crystal structure of urease from *S. pasteurii* was downloaded from the PDB (PDB id: 4UBP at 1.55 Å resolution). The crystal structures of jack bean (4GY7) and *S. pasteurii* urease (4UBP) were aligned using Chimera [33] with an rmsd of 0.6, which indicates good alignment of the conserved residues in the active site of both structures.

The docked conformation of most active urease inhibitor **4e** against urease from *S. pasteurii* is given in Fig. 8. Similar binding mode was observed as that in jack bean urease. The compound was found to bind at the entrance of the active site and was found to have a snug fit. Cys322 is a highly conserved residue among bacterial ureases, this

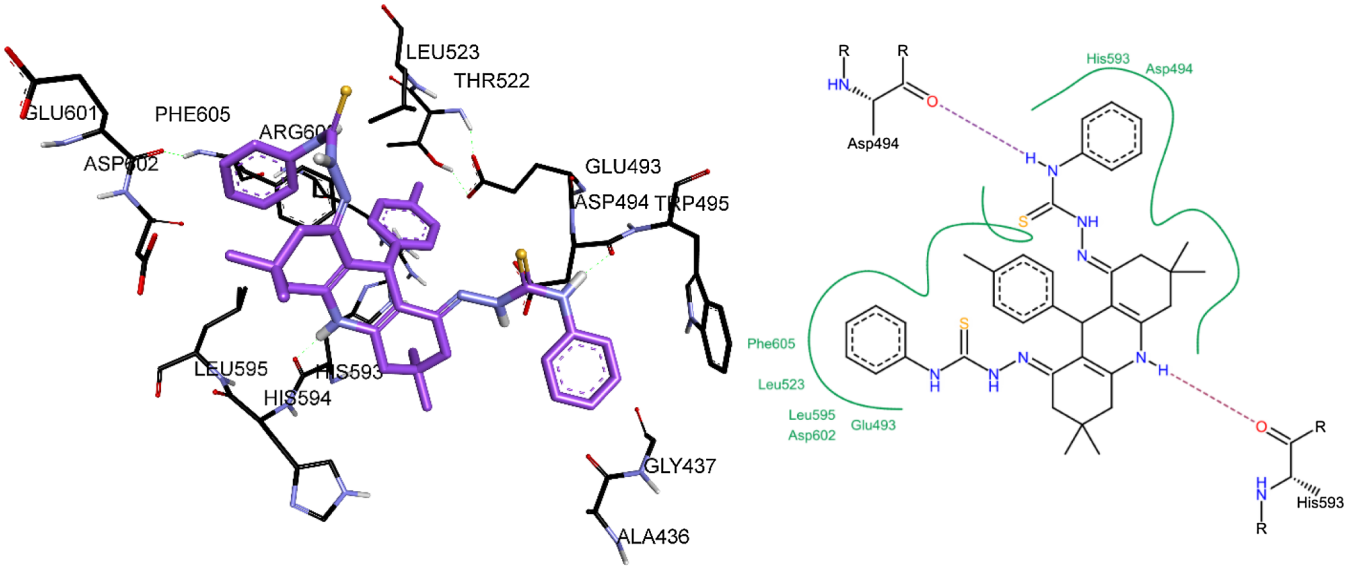

Fig. 6. 3D (left) and 2D (right) interactions of docked conformation of **4e**.

residue is important since it forms the part of the mobile flap at the entrance of active site and is essential for urease catalytic activity. It has been previously shown that covalent binding of benzoquinone [34] and benzisoselenazol [35] derived compounds to this cysteine residue results in irreversible inhibition of this enzyme. Herein compound **4e** was found to bind at the entrance of the active site, the NH groups of the thiourea linkage was making a hydrogen bond with Cys322 (Fig. 8), this probably indicates that the binding of acridine derivatives against *S. pasteurii* urease might be irreversible. Other hydrogen bonded interactions were also observed. The NH group of the acridine ring was found to make hydrogen bond with Ala366.

Similarly, compound **6d** was also docked against *S. pasteurii* urease enzyme, as shown in Fig. 9. Unlike compound **4e**, in compound 6d there was no direct hydrogen bond with Cys322, however one of the nitro group was found to be in direct contact with Ni metal ions in the active site. In addition the nitro groups were also found to be involved in extensive hydrogen bond networks, making hydrogen bonds with His323, His222, and Arg339.

4.1. *In-Silico ADME evaluation*

In order to determine drug-likeness of compounds (**4a-4e** and **6a-6l**), *in silico* calculation of some physiochemical parameters was carried out (OSIRIS 4.7.2) [36], as shown in Table 3. cLogP is the octanol water partition coefficient, which is the ratio of concentration of compound in octanol to its concentration in water. This is a very valuable parameter since it provides an estimate of ability of a compound to move/cross from aqueous phase to lipid phase, hence providing a measure of ability of compounds to cross the cell membranes. One of the key parameters for success of drug molecules is their water solubility, clogS is a

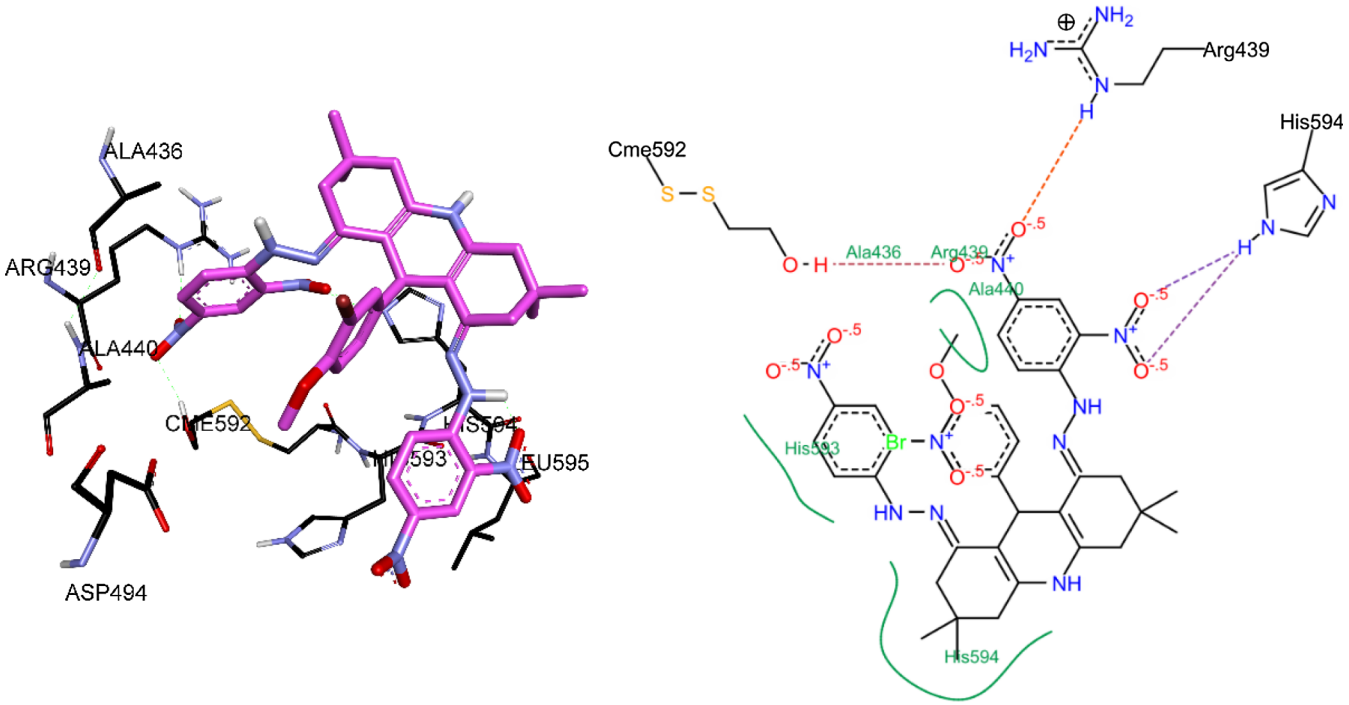

Fig. 7. 3D (left) and 2D (right) interactions of docked conformation of **6d**.

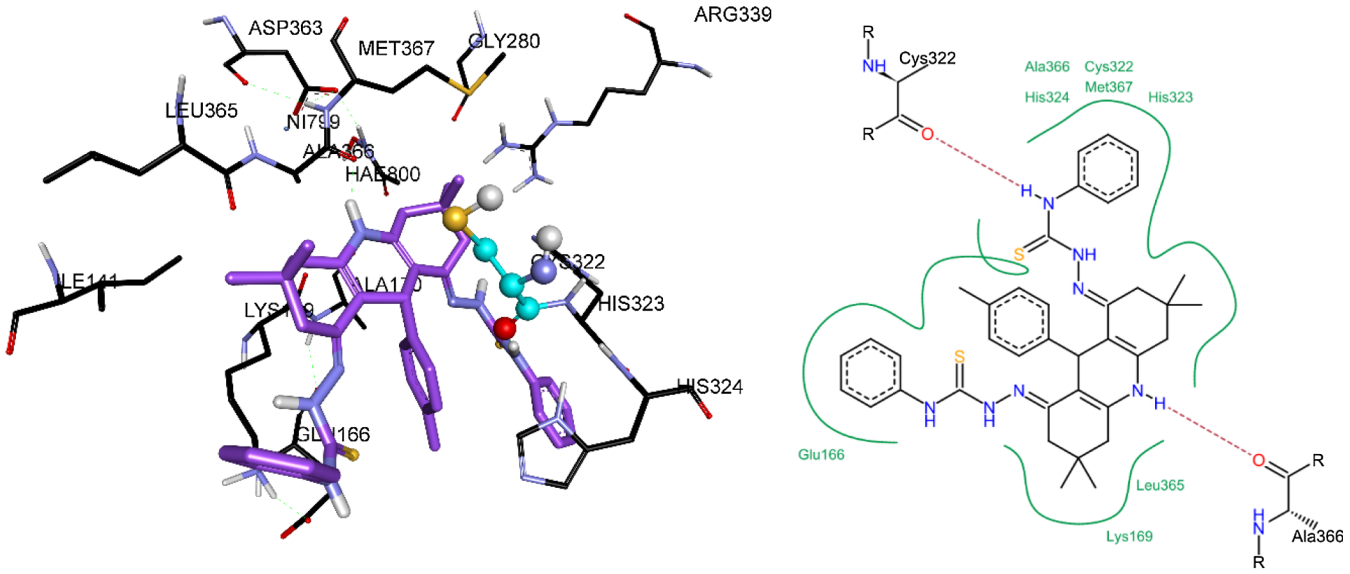

Fig. 8. 3D (left) and 2D (right) interactions of docked conformation of **4e**. The Cys322, which forms part of the mobile flap of active site, is represented in cyan color with ball and stick representation.

measure of water solubility of compounds in water in mol/L at 25 °C, and at pH of 7.5. Total number of hydrogen bond donors (HD) and hydrogen bond acceptors (HA) should not be greater than 5 and 10, respectively. As can be seen from the Table 3, only **4d** and **4e** had hydrogen bond donors of 6, all other compounds had HD in the range 3–5. Similarly, for number of hydrogen bond acceptors, compounds from first series, that is **4a-4e** had HA in the range 7–9, however, for all compounds of second series (**6a-6l**), HA was 17–18. Polar surface area (PSA) is sum of all polar atoms in a molecule. It provides an estimate of ability of a compound to cross blood brain barrier (BBB). Ideally PSA should be less than 140, only two compounds **4a** and **4b**, had PSA less than 140. Only three compounds **4c**, **4d** and **4e**, were predicted to be highly mutagenic and tumorigenic. No such effect was predicted for all other compounds from both series.

5. Conclusion

Two series of acridine derivatives were synthesized by first preparing an acridinedione scaffold, which was further reacted with hydrazine to yield acridinehydrazones, which were reacted with different (thio)semicarbazides to yield acridine (thio)semicarbazones (**4a-4e**). Similarly compounds **6a-6l** were synthesized by reacting different acridinediones to substituted phenylhydrazine. All synthesized compounds were evaluated for their inhibitory potential against urease enzyme *in vitro*. All compounds were found to be active against urease, best inhibitory activity was exhibited by compounds **4e** and **6d**. In order to rationalize the binding modes of most active inhibitors, molecular docking studies were carried out. It was found that due to the bulky nature of the molecules, they prefer to bind at the entrance of the active site of enzyme and do not make any direct contact with the

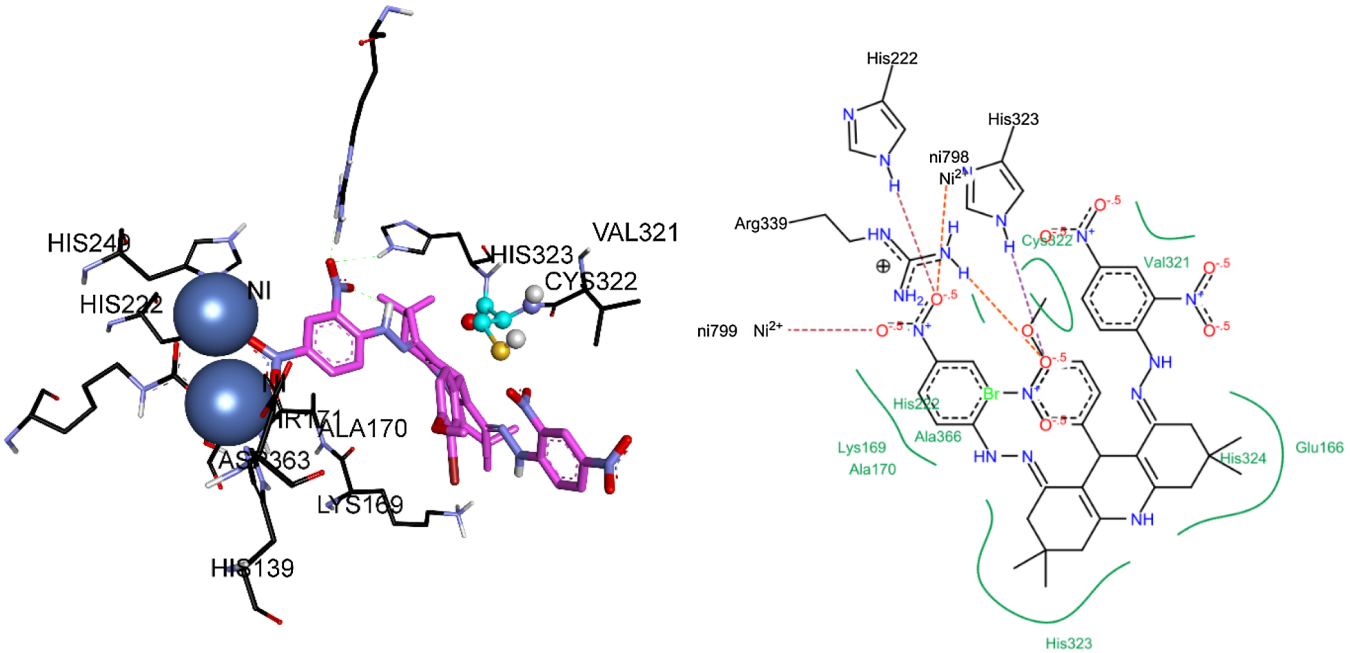

Fig. 9. 3D (left) and 2D (right) interactions of docked conformation of **6d**. The Cys322, which forms part of the mobile flap of active site, is represented in cyan color with ball and stick representation.

Table 3
In silico calculation of some ADME parameters for compounds **4a-4e** and **6a-6l**.

Entry	Compound	cLogP	cLogS	HA	HD	PSA	Mutagenic	Tumorigenic
1	**4a**	9.1561	−10.862	9	5	119.01	None	None
2	**4b**	9.7621	−11.598	9	5	119.01	None	None
3	**4c**	9.0814	−9.902	7	5	149.05	High	High
4	**4d**	8.3918	−9.262	8	6	169.28	High	High
5	**4e**	8.5934	−9.89	8	6	169.28	High	High
6	**6a**	7.8924	−9.398	17	3	244.09	None	None
7	**6b**	7.6493	−9.368	17	3	244.09	None	None
8	**6c**	8.1545	−9.79	17	3	244.09	None	None
9	**6d**	8.1545	−9.79	17	3	244.09	None	None
10	**6f**	7.6493	−9.368	17	3	244.09	None	None
11	**6g**	8.2037	−9.906	18	3	253.32	None	None
12	**6h**	7.5793	−9.386	18	3	253.32	None	None
13	**6i**	7.5793	−9.386	18	3	253.32	None	None
14	**6j**	7.4785	−9.072	18	3	253.32	None	None
15	**6k**	7.4785	−9.072	18	3	253.32	None	None
16	**6l**	7.2028	−8.758	18	4	264.32	None	None

catalytic Ni metal ions. In order to have an estimate of ability of these compounds to inhibit urease enzyme of a pathogen bacterium *S. Pasteurii*, molecular docking studies against urease enzyme from *S. Pasteurii* were also carried out. Compounds were found to have favorable binding affinity, indicating potential usefulness of such compounds for targeting pathogenic urease enzyme.

6. Experimental

All the starting materials include dimedone, benzaldehyde, ammonium acetate, phenyl hydrazines, (thio)isocynate *etc*. were purchased from different commercial suppliers and used without further purification. Analytical grade solvents were used for reactions and purification purposes where needed. All the reactions were monitored by using thin layer chromatography (TLC) with silica gel aluminium backed plates. They spot of compounds were visualised by exposing to UV light (254 nm) or with potassium permanganate or vanillin as appropriate. The NMR spectra were obtained as dilute solutions in the appropriate solvent at 25 °C unless otherwise stated. ^{1}H and ^{13}C NMR spectra were recorded at 300 MHz, or 400 MHz as indicated. The chemical shifts values were recorded on the δ scale (ppm) using residual solvent as an internal standard ($CDCl_3$: δ_H 7.26, δ_C 77.0; d_6-DMSO: δ_H 2.50, δ_C 39.43; D_3COD: δ_H 3.31, δ_C 49.05, etc.) [37]. All coupling constants were reported in Hertz (Hz) and multiplicities were labelled s (singlet), d (doublet), t (triplet), q (quartet), quint (quintet), sex (sextuplet), and where necessary the prefixes br (broad) or app (apparent) were used. Infrared spectra were recorded as solid on KBr disc or dilute solutions in appropriate solvent unless otherwise stated. Absorptions were labelled s (strong), m (medium), w (weak), and where necessary were supplemented with the suffix br (broad). Mass spectra were recorded using electrospray (ES+) or chemical ionisation (CI+), Fast atom bombardment (FAB^+), and Matrix-assisted laser desorption/ionization (MALDI) techniques.

6.1. Molecular modeling and docking studies

Crystal structures of jack bean and *S. pasteurii* urease were downloaded from the Protein Data Bank (PDB ids: 4GY7 and 4UBP) at a resolution of 1.49 Å and 1.55 Å, respectively. The structures of compounds were optimized using semi-empirical PM3 method in HyperChem [38]. Docking was carried out using BioSolveIT's LeadIT software [39] that makes use of the versatile FlexX docking procedure. Docked conformations were visualized using Discovery Studio Visualizer 4.0 [40].

6.2. General procedure for the synthesis of Acridine-based (thio) semicarbazones (4a-4e) and hydrazones (6a-6l)

In a typical reaction, an oven dried round bottomed flask was cooled to room temperature and charged with dimedone (10 mmol, 1.40 g), corresponding benzaldehyde (0.50 mL, 5 mmol), ammonium acetate (0.57 g, 7.5 mmol), nickel (II) fluoride tetrahydrate (25 mol%) as catalyst and ethanol (3 mL). The resulting reaction mixture was heated at reflux (78–80 °C) for 1.5 h, cooled, dissolved in methanol and poured into the crushed ice in a beaker. The mixture was further stirred to dissolve catalyst and to precipitate out corresponding acridine-based product **2** which was filtered, dried and washed in *n*-hexane to remove the un-reacted benzaldehyde to afford pure corresponding acridine **2** in 86% yield (1.50 g) [32].

Synthesis of Acridin-based (thio)semicarbazones ***(4a-4e)*****;** The obtained acridine compound **2** (2 mmol, 0.69 g) was then treated with excess of hydrazine hydrate (10 mL) and protonated acid *i.e*. acetic acid (2 mL) as catalyst at 120 °C until the complete consumption of starting material, monitored by TLC analysis with eluents mixture (EtOAc:Hexane, 3/7). The reaction mixture was diluted with water to get precipitate compound **3** which was filtered and dried under vacuum to get intermediate **3a** for further reaction with corresponding phenylisocyanate or phenyl isothiocyanate. The hydrazine group bearing intermediate **3** (1.0 equiv, 0.378 g) was reacted with corresponding iso (thio)cynate (*m*-chlorophenyl isocyanate) (2 mmol, 0.24 mL) at 100 °C overnight in acetonitrile (15 mL) as solvent. The reaction mixture was cooled down at ambient temperature resulting in the formation of precipitates. The precipitates were filtered, washed with warm acetonitrile and dried to obtain the pure compound **4a** (0.452 g; 63% yield). The other compounds of series **4a-4e** were also obtained in variable yields Scheme 1.

Synthesis of Acridine-based hydrazones ***(6a-6l)***; The corresponding acridine-based compound **2** (0.6 mmol, 0.218 g) was treated with *o,p*-dinitrophenyl hydrazine (2 mmol, 0.396 g) in the presence of H_2SO_4 (1 mL) in MeOH (3 mL). The reaction mixture was heated at reflux until the complete consumption of starting materials. The reaction mixture was diluted with water to get precipitate compound **6a** which was filtered and dried under vacuum. The yield for **6a** was obtained 96% (0.415 g) and in the similar way the other compounds of series **6a-6l** were obtained in different yields Scheme 1.

6.3. Spectral data

6.3.1. 2,2′-((1E,8E)-3,3,6,6-Tetramethyl-9-phenyl-3,4,6,7,9,10-hexahydroacridine-1,8(2H,5H)-diylidene)bis(N-(m-chlorophenyl)hydrazine-1-carbothioamide) (4a)

Greenish solid, yield 63% (453 mg), M.P. 282–285 °C; IR (ν_{max},

cm^{-1}): (KBr disc, solid) 3411, 3330, 3181, 3094, 2957, 1683, 1588, 1525, 1482, 1424, 1298, 1241, 1102, 1001, 879, 762, 688, 639. ^{1}H NMR (400 MHz, DMSO-d_6): δ_H 9.35 (2H, brs, 2N*H*), 8.75 (2H, brs, 2N*H*), 8.43 (1H, brs, N*H*), 7.84 (2H, brs, Ar*H*), 7.46 (2H, app d, J = 7.2 Hz, Ar*H*), 7.30 (2H, brs, Ar*H*), 7.06 (4H, app t, J = 6.8 Hz, Ar*H*), 6.99–6.95 (3H, m, Ar*H*), 5.38 (1H, s, C*H*), 2.30 (4H, app t, J = 16.4 Hz, $2CH_2$), 2.09 (4H, app t, J = 17.0 Hz, $2CH_2$), 1.03 (6H, s, $2CH_3$), 0.80 (6H, s, $2CH_3$); ^{13}C NMR (100 MHz, DMSO-d_6): δ_C 153.3 (C), 148.8 (C), 148.5 (C), 140.7 (C), 137.8 (C), 133.2 (C), 130.1 (CH), 128.1 (CH), 127.3 (CH), 125.2 (CH), 121.6 (CH), 118.1 (CH), 117.1 (CH), 106.5 (C), 39.5 (CH_2 × 2), 37.7 (CH_2 × 2), 35.7 (CH), 30.3 (C), 29.5(CH_3 × 2), 26.7 (CH_3 × 2). ESI-MS *m/z*, 684.6 (M + H); ESI-HRMS *m/z* $C_{37}H_{40}Cl_2N_7O_2$ (M + H) Found 684.2615, Calculated 684.2619.

6.3.2. 2,2′-((1E,8E)-3,3,6,6-Tetramethyl-9-(p-chlorophenyl)-3,4,6,7,9,10-hexahydroacridine-1,8(2H,5H)-diylidene)bis(N-(m-chlorophenyl)hydrazine-1-carbothioamide) (4b)

Greenish solid, yield 50% (426 mg), M.P. 329.3–332 °C; IR (ν_{max}, cm^{-1}): (KBr disc, solid) 3633, 3420, 3343, 3104, 2957, 2926, 1758, 1632, 1589, 1524, 1482, 1424, 1380, 1294, 1250, 1223, 1158, 1096, 1008, 881, 765, 681, 644. ^{1}H NMR (400 MHz, DMSO-d_6): δ_H 9.34 (2H, brs, 2N*H*), 8.78 (2H, brs, 2N*H*), 8.44 (1H, brs, N*H*), 7.87 (2H, brs, Ar*H*), 7.48 (2H, app brs, Ar*H*), 7.30 (2H, app brs, Ar*H*), 7.11 (2H, app brs, Ar*H*), 6.99 (1H, m, Ar*H*), 6.87 (2H, m , Ar*H*), 5.43 (1H, s, C*H*), 2.30 (4H, app t, J = 16.8 Hz, $2CH_2$), 2.09 (4H, app t, J = 16.4 Hz, $2CH_2$), 1.03 (6H, s, $2CH_3$), 0.80 (6H, s, $2CH_3$). MALDI-MS *m/z*, 717.09 (M^+), 718, 719, 720.

6.3.3. 2,2′-((1E,8E)-9-(m-hydroxyphenyl)-3,3,6,6-tetramethyl-3,4,6,7,9,10-hexahydroacridine-1,8(2H,5H)-diylidene)bis(N-phenylhydrazine-1-carbothioamide) (4c)

Golden yellow solid, yield 60% (518 mg), M.P. 278–281 °C; IR (ν_{max}, cm^{-1}): (KBr disc, solid) 3270, 3216, 3091, 3091, 2953, 1645, 1596, 1529, 1479, 1406, 1365, 1322, 1241, 1192, 1075, 999, 929, 775, 699. ^{1}H NMR (400 MHz, DMSO-d_6): δ_H 10.21 (2H, brs, 2N*H*), 9.43 (2H, brs, 2N*H*), 9.09 (1H, s, ArO*H*), 8.80 (1H, brs, N*H*), 7.46 (4H, app d, J = 7.6 Hz, Ar*H*), 7.20–7.10 (6H, m, Ar*H*), 6.91 (1H, d, J = 6.0 Hz, ArH), 6.68 (1H, s, Ar*H*), 6.63 (1H, t, J = 7.6 Hz, Ar*H*), 6.34 (1H, d, J = 6.8 Hz, Ar*H*), 5.22 (1H, s, C*H*), 2.49 (2H, obscured by DMSO signal, CH_2), 2.33 (2H, d, J = 16.2 Hz, CH_2), 2.26 (2H, d, J = 16.8 Hz, Ar*H*), 2.14 (2H, d, J = 16.8 Hz, CH_2), 1.04 (6H, s, $2CH_3$), 0.83 (6H, s, $2CH_3$). ESI-MS *m/z*, 664.1 (M + H); ESI-HRMS *m/z* $C_{37}H_{42}N_7OS_2$ (M + H) Found 664.2887, Calculated 664.2900.

6.3.4. 2,2′-((1E,8E)-9-(m-hydroxyphenyl)-3,3,6,6-tetramethyl-3,4,6,7,9,10-hexahydroacridine-1,8(2H,5H)-diylidene)bis(N-(o-fluorophenyl)hydrazine-1-carbothioamide) (4d)

Golden yellow solid, yield 76% (456 mg), M.P. 286–288 °C; IR (ν_{max}, cm^{-1}): (KBr disc, solid) 3270, 3219, 3148, 3090, 2950, 2892, 1648, 1598, 1530, 1477, 1405, 1365, 1322, 1236, 1098, 1001, 941, 879, 755, 713, 755, 713, 633, 587. ^{1}H NMR (400 MHz, DMSO-d_6): δ_H 10.39 (2H, brs, 2N*H*), 9.14 (2H, brs, 2N*H*), 8.99 (1H, s, ArO*H*), 8.82 (1H, brs, N*H*), 7.65 (2H, t, J = 7.2 Hz, Ar*H*), 7.22–7.20 (2H, m, Ar*H*), 7.10 (2H, app t, J = 7.4 Hz, Ar*H*), 6.94 (2H, t, J = 9.2 Hz, Ar*H*), 6.82 (1H, d, J = 6.8 Hz, Ar*H*), 6.60 (1H, s, Ar*H*), 6.52 (1H, t, J = 7.6 Hz, Ar*H*), 6.29 (1H, d J = 8.0 Hz, Ar*H*), 5.12 (1H, s, C*H*), 2.49 (2H, obscured by DMSO signal, CH_2), 2.32 (2H, d, J = 16.4 Hz, CH_2), 2.26 (2H, d, J = 16.4 Hz, Ar*H*), 2.14 (2H, d, J = 16.4 Hz, CH_2), 1.07 (6H, s, $2CH_3$), 0.84 (6H, s, $2CH_3$); ^{13}C NMR (75 MHz, DMSO-d_6): δ_C 175.8 (C), 157.7 (C), 157.59/154.33 (C, $J_{c\text{-}f}$ = 244.5), 152.4 (C), 149.9 (C), 139.9 (C), 128.1 (CH), 126.9/126.8 (CH), 126.6/126.5 (C), 123.7 (CH), 119.5 (CH), 115.3/115.0 (CH), 114.6 (CH), 112.3 (CH), 106.6 (C), 39.5 (CH_2 × 2), 38.3 (CH_2 × 2), 35.9 (CH), 30.4 (C), 29.3 (CH_3 × 2), 26.5 (CH_3 × 2). MALDI-MS *m/z*, 699.1 (M^+), 700.1; ESI-HRMS *m/z* $C_{37}H_{40}F_2N_7OS_2$ (M + H) Found 700.2698, Calculated 700.2705.

6.3.5. 2,2′-((1E,8E)-3,3,6,6-Tetramethyl-9-(p-mthylphenly)-3,4,6,7,9,10-hexahydroacridine-1,8(2H,5H)-diylidene)bis(N-phenylhydrazine-1-carbothioamide) (4e)

Yellow solid, yield 74% (487 mg), M.P. 235–239 °C; IR (ν_{max}, cm^{-1}): (KBr disc, solid) 3662, 3452, 3303, 2955, 2920, 1649, 1594, 1522, 1475, 1406, 1368, 1324, 1240, 1190, 1076, 1016, 930, 841, 780, 753, 694. ^{1}H NMR (400 MHz, DMSO-d_6): δ_H 10.15 (2H, brs, 2N*H*), 9.47 (2H, brs, 2N*H*), 8.76 (1H, brs, N*H*), 7.44–7.42 (4H, m, Ar*H*), 7.25–7.24 (6H, m, Ar*H*), 7.14 (2H, d, J = 6.8 Hz, Ar*H*), 6.76 (2H, d, J = 7.6 Hz, Ar*H*), 5.30 (1H, s, C*H*), 2.44 (2H, obscured by DMSO signal, CH_2), 2.32 (2H, d, J = 16.0 Hz, CH_2), 2.22 (2H, d, J = 16.4 Hz, Ar*H*), 2.13 (2H, d, J = 18.4 Hz, CH_2), 2.06 (3H, s, CH_3), 1.03 (6H, s, $2CH_3$), 0.80 (6H, s, $2CH_3$). ESI-MS *m/z*, $C_{38}H_{44}N_7S_2$ (M + H) Found 662.3098, Calculated 662.3094.

6.3.6. (1E,8E)-1,8-bis(2-(o,p-4-Dinitrophenyl)hydrazono)-3,3,6,6-tetramethyl-9-(4-methylphenyl)-1,2,3,4,5,6,7,8,9,10-decahydroacridine (6a)

Chocolate solid, yield 96% (415 mg), M.P. 280–285 °C; IR (ν_{max}, cm^{-1}): (KBr disc solid) 3405, 3311, 3104, 2960, 1615, 1489, 1425, 1335, 1267, 1219, 1139, 1059, 1011, 918, 834, 740, 678, 639. ^{1}H NMR (400 MHz, DMSO-d_6): δ_H 11.06 (2H, brs, 2N*H*), 9.20 (1H, brs, N*H*), 8.85 (2H, s, Ar*H*), 8.60 (2H, d, J = 10.4, Ar*H*), 7.95 (2H, d, J = 9.6, Ar*H*), 7.30 (2H, d, J = 8.0, Ar*H*), 7.03 (2H, d, J = 7.2, Ar*H*), 5.27 (1H, s, C*H*), 2.42 (2H, d, J = 16.8 Hz, $2CH_2$), 2.34 (2H, d, J = 15.6 Hz, CH_2), 2.20 (2H, d, J = 17.2 Hz, CH_2), 2.13 (3H, s, CH_3), 2.10 (2H, d, obscured by CH_3 group, CH_2), 1.10 (6H, s, $2CH_3$), 0.84 (6H, s, $2CH_3$). EI-MS *m/z*, 721.3 (M − 2H); EI-HRMS *m/z* $C_{36}H_{35}N_9O_8$ (M − 2H) Found 721.2622, Calculated 721.2609.

6.3.7. 3-((1E,8E)-1,8-bis(2-(o,p-Dinitrophenyl)hydrazono)-3,3,6,6-tetramethyl-1,2,3,4,5,6,7,8,9,10-decahydroacridin-9-yl)phenol (6b)

Chocolate solid, yield 85% (369 mg), M.P. 254–259 °C; IR (ν_{max}, cm^{-1}): (KBr disc solid) 3306, 3105, 2960, 1615, 1592, 1490, 1452, 1335, 1267, 1222, 1134, 1058, 920, 832, 741, 705, 584. ^{1}H NMR (400 MHz, DMSO-d_6): δ_H 11.06 (2H, brs, 2N*H*), 9.12 (1H, brs, N*H*), 8.85 (2H, d, J = 2.8 Hz, Ar*H*), 8.51 (2H, dd, J = 2.4, 9.6 Hz, Ar*H*), 7.92 (2H, d, J = 9.6 Hz, Ar*H*), 6.99 (1H, t, J = 7.6 Hz, Ar*H*), 6.87 (1H, s, Ar*H*), 6.83 (1H, d, J = 7.6 Hz, Ar*H*), 6.39 (1H, d, J = 6.4 Hz, Ar*H*), 5.20 (1H, s, C*H*), 2.50–2.40 (4H, m, $2CH_2$), 2.33 (2H, d, J = 15.6 Hz, CH_2), 2.20 (2H, d, J = 16.8 Hz, CH_2), 1.11 (6H, s, $2CH_3$), 0.84 (6H, s, $2CH_3$). EI-MS *m/z*, 723.2 (M − 2H); EI-HRMS *m/z* $C_{35}H_{33}N_9O_9$ (M − 2H) Found 723.2399, Calculated 723.2401.

6.3.8. (1E,8E)-1,8-bis(2-(o,p-Dinitrophenyl)hydrazono)-9-(p-fluorophenyl)-3,3,6,6-tetramethyl-1,2,3,4,5,6,7,8,9,10-decahydroacridine (6c)

Chocolate solid, yield 78% (339 mg), M.P. 284–290 °C; IR (ν_{max}, cm^{-1}): (KBr disc solid) 3631, 3419, 3357, 3291, 2959, 2369, 1618, 1589, 1480, 1424, 1371, 1329, 1253, 1216, 1129, 1092, 999, 920, 833, 743, 682, 608. ^{1}H NMR (400 MHz, DMSO-d_6): δ_H 11.05 (2H, brs, 2N*H*), 9.18 (1H, brs, N*H*), 8.85 (2H, s, Ar*H*), 8.60 (2H, d, J = 8.0 Hz, Ar*H*), 7.88 (2H, d, J = 9.6 Hz, Ar*H*), 7.42 (2H, t, J = 8.0 Hz, Ar*H*), 7.09–7.04 (2H, m, Ar*H*), 5.29 (1H, s, C*H*), 2.50–2.40 (4H, m, $2CH_2$), 2.33 (2H, d, J = 16.0 Hz, CH_2), 2.22 (2H, d, J = 16.4 Hz, CH_2), 1.11 (6H, s, $2CH_3$), 0.84 (6H, s, $2CH_3$); ^{13}C NMR (150 MHz, DMSO-d_6): δ_C 161.08/159.48 (C, $J_{c\text{-}f}$ = 240.0), 154.8 (C), 143.9 (C), 143.6 (C), 140.41 (C), 130.3 (CH), 129.91/129.86 (CH), 128.6 (C), 123.3 (CH), 115.7 (CH), 114.3/114.1 (CH), 107.3 (C), 39.1 (CH_2), 37.2 (CH_2), 35.1 (CH), 30.5 (C), 29.6 (CH_3 × 2), 26.3 (CH_3 × 2). EI-MS *m/z*, 727.6 (M^+), 725.4 (M − 2H); EI-HRMS *m/z* $C_{35}H_{32}N_9O_8F$ (M − 2H) Found 725.2390, Calculated 725.2358.

6.3.9. (1E,8E)-9-(m-Bromo-p-methoxyphenyl)-1,8-bis(2-(2,4-dinitrophenyl) hydrazono)-3,3,6,6-tetramethyl-1,2,3,4,5,6,7,8,9,10-decahydroacridine (6d)

Chocolate crystalline, yield 85% (417 mg), M.P. 274–279 °C; IR (ν_{max}, cm^{-1}): (KBr disc solid) 3693, 3383, 3302, 3095, 2955, 2922, 2369, 1730, 1619, 1588, 1479, 1420, 1333, 1249, 1124, 1053, 1020,

921, 880, 827, 742, 679. ^{1}H NMR (400 MHz, DMSO-d_6): δ_H 11.05 (2H, brs, 2N*H*), 9.18 (1H, brs, N*H*), 8.85 (2H, s, Ar*H*), 8.60 (2H, d, J = 8.0 Hz, Ar*H*), 7.88 (2H, d, J = 9.2 Hz, Ar*H*), 7.63 (1H, s, Ar*H*), 7.34 (1H, d, J = 6.8 Hz, Ar*H*), 7.01 (1H, d, J = 8.4 Hz, Ar*H*), 5.23 (1H, s, C*H*), 3.72 (3H, s, OCH_3), 2.50–2.31 (6H, m, $2CH_2$), 2.22 (2H, d, J = 16.8 Hz, CH_2), 1.11 (6H, s, $2CH_3$), 0.87 (6H, s, $2CH_3$). EI-MS *m/z*, 817.3 (M^+), 815.3 (M − 2H); EI-HRMS *m/z* $C_{36}H_{34}N_9O_9Br$ (M − 2H) Found 815.1669, Calculated 815.1663.

6.3.10. (1E,8E)-9-(p-Chlorophenyl)-1,8-bis(2-(o,p-dinitrophenyl) hydrazono)-3,3,6,6-tetramethyl-1,2,3,4,5,6,7,8,9,10-decahydroacridine (6e)

Chocolate solid, yield 75% (332 mg), M.P. 266–270 °C; IR (ν_{max}, cm^{-1}): (KBr disc solid) 3784, 3357, 3308, 3102, 2958, 1618, 1589, 1481, 1423, 1369, 1332, 1257, 1216, 1131, 1058, 1004, 920, 833, 744, 790, 582. ^{1}H NMR (400 MHz, DMSO-d_6): δ_H 11.05 (2H, brs, 2N*H*), 9.18 (1H, brs, N*H*), 8.85 (2H, d, J = 2.4 Hz, Ar*H*), 8.60 (2H, d, J = 7.6 Hz, Ar*H*), 7.88 (2H, d, J = 9.6 Hz, Ar*H*), 7.43 (2H, t, J = 7.2 Hz, Ar*H*), 7.07 (1H, t, J = 8.4 Hz, Ar*H*), 5.32 (1H, s, C*H*), 2.50–2.31 (6H, m, $3CH_2$), 2.22 (2H, d, J = 16.8 Hz, CH_2), 1.11 (6H, s, $2CH_3$), 0.84 (6H, s, $2CH_3$). EI-MS *m/z*, 741.2 (M − 2H).

6.3.11. (1E,8E)-1,8-bis(2-(o,p-Dinitrophenyl)hydrazono)-3,3,6,6-tetramethyl-9-(p-(methylthio)phenyl)-1,2,3,4,5,6,7,8,9,10-decahydroacridine (6f)

Chocolate solid, yield 71% (321 mg), M.P. 267–271 °C; IR (ν_{max}, cm^{-1}): (KBr disc solid) 3707, 3354, 3300, 3099, 2957, 2922, 2369, 1615, 1587, 1482, 1421, 1329, 1251, 1218, 1126, 919, 833, 740, 690, 581. ^{1}H NMR (400 MHz, DMSO-d_6): δ_H 11.05 (2H, brs, 2N*H*), 9.14 (1H, brs, N*H*), 8.85 (2H, d, J = 2.4 Hz, Ar*H*), 8.60 (2H, d, J = 7.6 Hz, Ar*H*), 7.91 (2H, d, J = 9.6 Hz, Ar*H*), 7.35 (2H, d, J = 8.0 Hz, Ar*H*), 7.13 (2H, d, J = 8.4 Hz, Ar*H*), 5.25 (1H, s, C*H*), 2.50–2.32 (6H, m, $3CH_2$), 2.20 (2H, d, J = 18.0 Hz, CH_2), 1.11 (6H, s, $2CH_3$), 0.85 (6H, s, $2CH_3$). EI-MS *m/z*, 755.3 (M^+), 753.3 (M − 2H); EI-HRMS *m/z* $C_{36}H_{35}N_9O_8S$ (M − 2H) Found 753.2308, Calculated 753.2284.

6.3.12. (1E,8E)-1,8-bis(2-(o,p-Dinitrophenyl)hydrazono)-9-(p-fluoro-m-methoxyphenyl)-3,3,6,6-tetramethyl-1,2,3,4,5,6,7,8,9,10-decahydroacridine (6g)

Chocolate solid, yield 97% (442 mg), M.P. 270–275 °C; IR (ν_{max}, cm^{-1}): (KBr disc solid) 3702, 3381, 3102, 2960, 1618, 1588, 1510, 1481, 1422, 1370, 1330, 1261, 1215, 1129, 1088, 1057, 921, 829, 746. ^{1}H NMR (400 MHz, DMSO-d_6): δ_H 11.09 (2H, brs, 2N*H*), 9.17 (1H, brs, N*H*), 8.86 (2H, s, Ar*H*), 8.56 (2H, d, J = 9.2 Hz, Ar*H*), 7.90 (2H, d, J = 9.6 Hz, Ar*H*), 7.11–7.04 (3H, m, Ar*H*), 6.94 (1H, brs, Ar*H*), 5.30 (1H, s, C*H*), 3.70 (3H, s, OCH_3), 2.50–2.32 (6H, m, $3CH_2$), 2.23 (2H, d, J = 16.4 Hz, CH_2), 1.11 (6H, s, $2CH_3$), 0.86 (6H, s, $2CH_3$); ^{13}C NMR (150 MHz, DMSO-d_6): δ_C 154.8 (C), 150.41/148.81 (C, $J_{c\text{-}f}$ = 240.0), 146.1/146.0 (C), 144.3 (C), 143.8 (C), 140.4 (C), 136.2 (C), 130.2 (CH), 128.7 (C), 123.4 (CH), 120.4 (C), 115.5 (CH), 115.01/114.88 (CH), 113.7 (CH), 107.2 (C), 55.82/55.70 (OCH_3), 39.1 (CH_2), 37.2 (CH_2), 35.6 (CH), 30.5 (C), 29.6 (CH_3 × 2), 26.3 (CH_3 × 2). EI-MS *m/z*, 755.1 (M − 2H); EI-HRMS *m/z* $C_{36}H_{34}N_9O_9F$ (M − 2H) Found 755.2464, Calculated 755.2462.

6.3.13. (1E,8E)-1,8-bis(2-(o,p-Dinitrophenyl)hydrazono)-9-(m-methoxyphenyl)-3,3,6,6-tetramethyl-1,2,3,4,5,6,7,8,9,10-decahydroacridine (6h)

Chocolate solid, yield 86% (381 mg), M.P. 205–210 °C; IR (ν_{max}, cm^{-1}): (KBr disc solid) 3703, 3450, 3102, 2959, 1615, 1490, 1428, 1335, 1246, 1222, 1135, 1058, 1008, 919, 832, 747, 704, 583. ^{1}H NMR (400 MHz, DMSO-d_6): δ_H 11.08 (2H, brs, 2N*H*), 9.15 (1H, brs, N*H*), 8.86 (2H, d, J = 2.4 Hz, Ar*H*), 8.53 (2H, d, J = 9.6 Hz, Ar*H*), 7.92 (2H, d, J = 8.4 Hz, Ar*H*), 7.14 (1H, t, J = 8.0 Hz, Ar*H*), 7.02 (1H, d, J = 7.2 Hz, Ar*H*), 6.94 (1H, s, Ar*H*), 6.58 (1H, d, J = 6.8 Hz, Ar*H*), 5.29 (1H, s, C*H*), 3.64 (3H, s, OCH_3), 2.50–2.31 (6H, m, $3CH_2$), 2.23 (2H, d, J = 16.4 Hz, CH_2), 1.11 (6H, s, $2CH_3$), 0.86 (6H, s, $2CH_3$). EI-HRMS *m/z* $C_{36}H_{35}N_9O_9$ (M − 2H)Found 737.2545, Calculated 737.2558.

6.3.14. (1E,8E)-1,8-bis(2-(o,p-Dinitrophenyl)hydrazono)-9-(p-methoxyphenyl)-3,3,6,6-tetramethyl-1,2,3,4,5,6,7,8,9,10-decahydroacridine (6i)

Chocolate solid, yield 82% (363 mg), M.P. 275–279 °C; IR (ν_{max}, cm^{-1}): (KBr disc solid) 3701, 3384, 3302, 3101, 2957, 1616, 1587, 1511, 1479, 1422, 1252, 1129, 1056, 920, 834, 742, 586. ^{1}H NMR (400 MHz, DMSO-d_6): δ_H 11.06 (2H, brs, 2N*H*), 9.09 (1H, brs, N*H*), 8.86 (2H, s, Ar*H*), 8.60 (2H, d, J = 8.8 Hz, Ar*H*), 7.92 (2H, d, J = 9.6 Hz, Ar*H*), 7.31 (2H, d, J = 8.0 Hz, Ar*H*), 6.79 (2H, d, J = 8.0 Hz, Ar*H*), 5.21 (1H, s, C*H*), 3.62 (3H, s, OCH_3), 2.50–2.34 (4H, m, $2CH_2$), 2.32 (2H, d, J = 16.0 Hz, CH_2), 2.20 (2H, d, J = 16.4 Hz, CH_2), 1.11 (6H, s, $2CH_3$), 0.86 (6H, s, $2CH_3$); ^{13}C NMR (400 MHz, DMSO-d_6): δ_C 157.1 (C), 154.6 (C), 143.9 (C), 140.9 (C), 139.6 (C), 136.1 (C), 130.4 (CH), 129.3 (CH), 128.5 (C), 123.3 (CH), 115.9 (CH), 112.8 (CH), 107.7 (C), 54.8 (CH_3), 39.3 (2 × CH_2), 37.2 (2 × CH_2), 34.9 (CH), 30.6 (C), 29.6 (2 × CH_3), 26.1 (2 × CH_3). EI-HRMS *m/z* $C_{36}H_{35}N_9O_9$ (M − 2H) Found 737.2563, Calculated 737.2558.

6.3.15. 4-((1E,8E)-1,8-bis(2-(o,p-Dinitrophenyl)hydrazono)-3,3,6,6-tetramethyl-1,2,3,4,5,6,7,8,9,10-decahydroacridin-9-yl)phenol (6j)

Red solid, yield 99% (433 mg), M.P. 206–211 °C; IR (ν_{max}, cm^{-1}): (KBr disc solid) 3784, 3449, 3311, 3105, 2959, 1615, 1509, 1489, 1428, 1336, 1264, 1225, 1135, 1058, 1004, 919, 837, 745, 710, 583. ^{1}H NMR (400 MHz, DMSO-d_6): δ_H 11.07 (2H, brs, 2N*H*), 9.07 (1H, brs, N*H*), 8.85 (2H, d, J = 2.8, Ar*H*), 8.60 (2H, dd, J = 2.4, 9.6 Hz, Ar*H*), 7.92 (2H, d, J = 9.6 Hz, Ar*H*), 7.19 (2H, d, J = 8.0 Hz, Ar*H*), 6.58 (2H, d, J = 8.0 Hz, Ar*H*), 5.17 (1H, s, C*H*), 2.50–2.30 (6H, m, $3CH_2$), 2.19 (2H, d, J = 16.4 Hz, CH_2), 1.11 (6H, s, $2CH_3$), 0.84 (6H, s, $2CH_3$). EI-HRMS *m/z* $C_{35}H_{33}N_9O_9$ (M − 2H) Found 723.2389, Calculated 723.2396.

6.3.16. (1E,8E)-9-(m-Chlorophenyl)-1,8-bis(2-(o,p-dinitrophenyl) hydrazono)-3,3,6,6-tetramethyl-1,2,3,4,5,6,7,8,9,10-decahydroacridine (6k)

Chocolate solid, yield 76% (339 mg), M.P. 284–288 °C; IR (ν_{max}, cm^{-1}): (KBr disc solid) 3784, 3356, 3101, 2958, 1616, 1586, 1478, 1420, 1330, 1252, 1218, 1129, 1090, 919, 828, 741, 699, 586. ^{1}H NMR (400 MHz, DMSO-d_6): δ_H 11.07 (2H, brs, 2N*H*), 9.07 (1H, brs, N*H*), 8.86 (2H, s, Ar*H*), 8.52 (2H, d, J = 9.6 Hz, Ar*H*), 7.84 (2H, d, J = 9.6 Hz, Ar*H*), 7.44 (1H, s, Ar*H*), 7.35 (1H, d, J = 7.6 Hz, Ar*H*), 7.29 (1H, t, J = 7.6 Hz, Ar*H*), 7.09 (1H, d, J = 7.2 Hz, Ar*H*), 5.28 (1H, s, C*H*), 2.39 (2H, obscured by DMSO signal, CH_2), 2.40 (2H, d, J = 15.6 Hz, CH_2), 2.32 (2H, d, J = 13.6 Hz, CH_2), 2.25 (2H, d, J = 16.4 Hz, CH_2), 1.11 (6H, s, $2CH_3$), 0.82 (6H, s, $2CH_3$). EI-HRMS *m/z* $C_{35}H_{32}N_9O_8Cl$ (M − 2H) Found 741.2055, Calculated 741.2062.

6.3.17. (1E,8E)-1,8-bis(2-(o,p-Dinitrophenyl)hydrazono)-9-(m-fluorophenyl)-3,3,6,6-tetramethyl-1,2,3,4,5,6,7,8,9,10-decahydroacridine (6l)

Chocolate solid, yield 81% (354 mg), M.P. 272–276 °C; IR (ν_{max}, cm^{-1}): (KBr disc solid) 3739, 3619, 3437, 3304, 3099, 2958, 2924, 1650, 1617, 1588, 1513, 1481, 1423, 1332, 1250, 1218, 1127, 1093, 1056, 920, 866, 828, 770, 741, 686, 592. ^{1}H NMR (400 MHz, DMSO-d_6): δ_H 11.07 (2H, brs, 2N*H*), 9.07 (1H, brs, N*H*), 8.86 (2H, s, Ar*H*), 8.57 (2H, d, J = 8.4 Hz, Ar*H*), 7.88 (2H, d, J = 9.2 Hz, Ar*H*), 7.32 (1H, s, Ar*H*), 7.6 (1H, d, J = 10.6 Hz, Ar*H*), 6.85 (1H, t, J = 6.8 Hz, Ar*H*), 5.37 (1H, s, C*H*), 2.49–2.31 (6H, m, $3CH_2$), 2.25 (2H, d, J = 16.8 Hz, CH_2), 1.11 (6H, s, $2CH_3$), 0.82 (6H, s, $2CH_3$); ^{13}C NMR (100 MHz, DMSO-d_6): δ_C 163.3/160.9 (C, $J_{c\text{-}f}$ = 241.0), 154.8 (C), 143.9 (C), 140.6 (C), 136.2 (C), 130.2 (CH), 129.25/129.18 (CH), 128.7 (C), 123.3 (CH), 115.7 (CH), 112.5/112.3/112.1 (CH), 106.9 (C), 39.1 (CH_2), 37.2 (CH_2), 35.1 (CH), 30.6 (C), 29.6 (CH_3 × 2), 26.2 (CH_3 × 2). EI-MS *m/z*, 725.0 (M − 2H); EI-HRMS *m/z* $C_{35}H_{32}N_9O_8F$ (M − 2H)

Found 725.2353, Calculated 725.2358.

7. Conflict of interest

Author(s) declared no conflict of interest.

Acknowledgement

We are thankful to Higher Education Commission, Pakistan for providing financial support of this project (HEC Project 5743 and 4732).

Appendix A. Supplementary material

Supplementary data to this article can be found online at https://doi.org/10.1016/j.bioorg.2018.09.032.

References

[1] H. Mobley, M.D. Island, R.P. Hausinger, Molecular biology of microbial ureases, Microbiol. Rev. 59 (1995) 451–480.
[2] D.L. Clemens, B.-Y. Lee, M.A. Horwitz, Purification, characterization, and genetic analysis of Mycobacterium tuberculosis urease, a potentially critical determinant of host-pathogen interaction, J. Bacteriol. 177 (1995) 5644–5652.
[3] I. Konieczna, P. Zarnowiec, M. Kwinkowski, B. Kolesinska, J. Fraczyk, Z. Kaminski, W. Kaca, Bacterial urease and its role in long-lasting human diseases, Curr. Protein Pept. Sci. 13 (2012) 789–806.
[4] K. Hirota, K. Nagata, Y. Norose, S. Futagami, Y. Nakagawa, H. Senpuku, M. Kobayashi, H. Takahashi, Identification of an antigenic epitope inhelicobacter pylori urease that induces neutralizing antibody production, Infect. Immun. 69 (2001) 6597–6603.
[5] B.E. Dunn, S.H. Phadnis, Structure, function and localization of Helicobacter pylori urease, Yale J. Biol. Med. 71 (1998) 63.
[6] D. Olivera-Severo, G.E. Wassermann, C. Carlini, Ureases display biological effects independent of enzymatic activity: is there a connection to diseases caused by urease-producing bacteria? Braz. J. Med. Biol. Res. 39 (2006) 851–861.
[7] C.-Y. Kao, B.-S. Sheu, J.-J. Wu, Helicobacter pylori infection: an overview of bacterial virulence factors and pathogenesis, Biomed. J. 39 (2016) 14–23.
[8] C. Follmer, Ureases as a target for the treatment of gastric and urinary infections, J. Clin. Pathol. 63 (2010) 424–430.
[9] C.S. Lieber, Gastritis and Helicobacter pylori: forty years of antibiotic therapy, Digestion 58 (1997) 203–210.
[10] H.L. Mobley, R. Belas, Swarming and pathogenicity of Proteus mirabilis in the urinary tract, Trends Microbiol. 3 (1995) 280–284.
[11] E. Hjelm, I. Lundell-Etherden, P.A. MÅRdh, Ascending urinary tract infections in rats induced by Staphylococcus saprophyticus and Proteus mirabilis, Acta Pathol. Microbiol. Immunol. Scand B 95 (1987) 347–350.
[12] D. Johnson, R. Russell, C. Lockatell, J. Zulty, J. Warren, H. Mobley, Contribution of Proteus mirabilis urease to persistence, urolithiasis, and acute pyelonephritis in a mouse model of ascending urinary tract infection, Infect. Immun. 61 (1993) 2748–2754.
[13] A. Martelli, P. Buli, V. Cortecchia, Urease Inhibitor Therapy in Infected Renal Stones, Advances in Nephrourology, Springer, 1981, pp. 431–439.
[14] K.-H. Bichler, E. Eipper, K. Naber, V. Braun, R. Zimmermann, S. Lahme, Urinary infection stones, Int. J. Antimicrob. Agents 19 (2002) 488–498.
[15] N.U. Rahman, M.V. Meng, M.L. Stoller, Infections and urinary stone disease, Curr. Pharm. Des. 9 (2003) 975–981.
[16] W.-K. Shi, R.-C. Deng, P.-F. Wang, Q.-Q. Yue, Q. Liu, K.-L. Ding, M.-H. Yang, H.-Y. Zhang, S.-H. Gong, M. Deng, 3-Arylpropionylhydroxamic acid derivatives as Helicobacter pylori urease inhibitors: synthesis, molecular docking and biological evaluation, Bioorg. Med. Chem. 24 (2016) 4519–4527.
[17] Z.-P. Xiao, Z.-Y. Peng, J.-J. Dong, R.-C. Deng, X.-D. Wang, H. Ouyang, P. Yang, J. He, Y.-F. Wang, M. Zhu, Synthesis, molecular docking and kinetic properties of β-hydroxy-β-phenylpropionyl-hydroxamic acids as Helicobacter pylori urease inhibitors, Eur. J. Med. Chem. 68 (2013) 212–221.
[18] C. Wei, M. Cohen, D. Swartz, S. Fernando, M. Corbett, Mutagenicity of some monoaromatic hydroxamic acids, Toxicol. Lett. 24 (1985) 111–116.
[19] W.S. Faraci, B.V. Yang, D. O'Rourke, R.W. Spencer, Inhibition of Helicobacter pylori urease by phenyl phosphorodiamidates: mechanism of action, Bioorganic Med. Chemi. Bioorg. Med. Chem. 3 (1995) 605–610.
[20] M. Steinmann, M. Wagner, F.R. Wurm, Poly (phosphorodiamidate) s by olefin metathesis polymerization with precise degradation, Chem. Eur. J. 22 (2016) 17329–17338.
[21] Y. Cui, X. Dong, Y. Li, Z. Li, W. Chen, Synthesis, structures and urease inhibition studies of Schiff base metal complexes derived from 3, 5-dibromosalicylaldehyde, Eur. J. Med. Chem. 58 (2012) 323–331.
[22] T.O. Brito, A.X. Souza, Y.C. Mota, V.S. Morais, L.T. de Souza, Â. de Fátima, F. Macedo, L.V. Modolo, Design, syntheses and evaluation of benzoylthioureas as urease inhibitors of agricultural interest, RSC Adv. 5 (2015) 44507–44515.
[23] A. Shakeel, A.A. Altaf, A.M. Qureshi, A. Badshah, Thiourea derivatives in drug design and medicinal chemistry: a short review, J. Drug. Des. Med. Chem. 2 (2016) 10–20.
[24] M.A.S. Aslam, S.-U. Mahmood, M. Shahid, A. Saeed, J. Iqbal, Synthesis, biological assay in vitro and molecular docking studies of new Schiff base derivatives as potential urease inhibitors, Eur. J. Med. Chem. 46 (2011) 5473–5479.
[25] S.U. Qazi, S.U. Rahman, A.N. Awan, M. Al-Rashida, R.D. Alharthy, A. Asari, A. Hameed, J. Iqbal, Semicarbazone derivatives as urease inhibitors: Synthesis, biological evaluation, molecular docking studies and in-silico ADME evaluation, Bioorg. Chem. 79 (2018) 19–26.
[26] A. Hameed, K.M. Khan, S.T. Zehra, R. Ahmed, Z. Shafiq, S.M. Bakht, M. Yaqub, M. Hussain, A.d.l.V. De León, N. Furtmann, Synthesis, biological evaluation and molecular docking of N-phenyl thiosemicarbazones as urease inhibitors, Bioorg. Chem. 61 (2015) 51–57.
[27] G.-H. Sheng, X.-F. Chen, J. Li, J. Chen, Y. Xu, Y.-W. Han, T. Yang, Z. You, H.-L. Zhu, Synthesis, Crystal Structures and Urease Inhibition of N'-(2-Bromobenzylidene)-2-(4-nitrophenoxy) acetohydrazide and N'-(4-Nitrobenzylidene)-2-(4-nitrophenoxy) acetohydrazide, Acta Chim. Slov. 62 (2015) 940–946.
[28] M.K. Rauf, A. Talib, A. Badshah, S. Zaib, K. Shoaib, M. Shahid, U. Floerke, J. Iqbal, Solution-phase microwave assisted parallel synthesis of N, N′-disubstituted thioureas derived from benzoic acid: biological evaluation and molecular docking studies, Eur. J. Med. Chem. 70 (2013) 487–496.
[29] W.A. Denny, Acridine derivatives as chemotherapeutic agents, Curr. Med. Chem. 9 (2002) 1655–1665.
[30] I. Antonini, P. Polucci, A. Magnano, B. Gatto, M. Palumbo, E. Menta, N. Pescalli, S. Martelli, Design, synthesis, and biological properties of new bis (acridine-4-carboxamides) as anticancer agents, J. Med. Chem. 46 (2003) 3109–3115.
[31] S. Uroos Qazi, S. Ur Rahman, A. Naz Awan, M. Al-Rashida, R.D. Alharthy, A. Asari, A. Hameed, J. Iqbal, Semicarbazone derivatives as urease inhibitors: synthesis, biological evaluation, molecular docking studies and in-silico ADME evaluation, Bioorg. Chem. (2018), https://doi.org/10.1016/j.bioorg.2018.1003.1029.
[32] I.O. Isaac, I. Munir, M. Al-Rashida, S.A. Ali, Z. Shafiq, M. Islam, R. Ludwig, K. Ayub, K.M. Khan, A. Hameed, Novel acridine-based thiosemicarbazones as 'turn-on' chemosensors for selective recognition of fluoride anion: a spectroscopic and theoretical study, R. Soc. Open Sci. 5 (2018) 180646.
[33] E.F. Pettersen, T.D. Goddard, C.C. Huang, G.S. Couch, D.M. Greenblatt, E.C. Meng, T.E. Ferrin, UCSF Chimera—a visualization system for exploratory research and analysis, J. Comput. Chem. 25 (2004) 1605–1612.
[34] L. Mazzei, M. Cianci, F. Musiani, S. Ciurli, Inactivation of urease by 1, 4-benzoquinone: chemistry at the protein surface, Dalton Trans. 45 (2016) 5455–5459.
[35] K. Macegoniuk, E. Grela, J. Palus, E. Rudzińska-Szostak, A. Grabowiecka, M. Biernat, Ł. Berlicki, 1, 2-Benzisoselenazol-3 (2 H)-one Derivatives As a New Class of Bacterial Urease Inhibitors, J. Med. Chem. 59 (2016) 8125–8133.
[36] T. Sander, J. Freyss, M. von Korff, C. Rufener, DataWarrior: an open-source program for chemistry aware data visualization and analysis, J. Chem. Inf. Model. 55 (2015) 460–473.
[37] G.R. Fulmer, A.J. Miller, N.H. Sherden, H.E. Gottlieb, A. Nudelman, B.M. Stoltz, J.E. Bercaw, K.I. Goldberg, NMR chemical shifts of trace impurities: common laboratory solvents, organics, and gases in deuterated solvents relevant to the organometallic chemist, Organometallics 29 (2010) 2176–2179.
[38] HyperChem(TM) Professional 8.0, Hypercube, Inc., 1115 NW 1114th Street, Gainesville, Florida 32601, USA.
[39] LeadIT v.2.1.8, BioSolveIT GmbH, Sankt Augustin, Germany, 2016. http://www.biosolveit.de.
[40] Accelrys Software Inc., Discovery Studio Modeling Environment, Release 4.0, Accelrys Software Inc., San Diego, CA, 2013.